

Invited

Transport Characteristics of Multiple Parallel Ballistic Point Contacts

Y.Hirayama

NTT Basic Research Laboratories,
3-9-11 Midori-Cho Tokyo 180

Multiple parallel ballistic point contacts are fabricated using the highly resistive region induced by focused Ga ion beam scanning. Total conductance of the fabricated structure in zero magnetic field is the sum of the conductance of each contact, and quantized characteristics are observed in the μA order. On the other hand, conductance of multiple parallel point contacts drastically decreases in a magnetic field. This conductance decrease originates from the novel type of magneto-depopulation accompanying ballistic circulating channels through pairs of contacts. Conductance oscillations corresponding to interference in circulating channels are also observed in the fabricated structures.

1.Introduction

Ballistic quantum point contacts (BPCs) have been successfully fabricated by means of split Schottky gates¹⁻³⁾ or ion implantation using focused ion beam^{4,5)}. Quantized conductance at the value of $G_i = 2e^2i/h$ (i : number of subbands in the BPC) has been reported for these structures. Ballistic transport experiments have been extended to series BPCs, in which two point contacts are placed in series within electron mean free path (l_e). It becomes clear that the total conductance of series BPCs is not $G_i/2$ but between $G_i/2$ and G_i as a function of separation and contact shapes^{3,6-8)}. Recently, C.G.Smith et al.⁹⁾ reported transport characteristics of double-parallel BPCs. However, systematic studies have not yet been carried out for multiple parallel BPC structures, where several point contacts are placed in parallel within l_e . In this paper, transport characteristics are discussed for multiple parallel BPCs with and without magnetic field.

2.Fabrication

A multiple parallel BPC structure was fabricated by scanning a focused Ga ion beam (Ga-FIB) across a rectangular mesa-etched pattern on an $\text{Al}_{0.3}\text{Ga}_{0.7}\text{As}/\text{GaAs}$ modulation doped wafer as shown in Fig.1. Starting wafers had carrier density of $(3-7) \times 10^{11} \text{cm}^{-2}$ and electron mobility of $(3-10) \times 10^5 \text{cm}^2/\text{Vs}$. The Ga-FIB scanning was followed by annealing at $700-770^\circ\text{C}$ for 15sec.. The depletion area around the implanted region defines the conductive channels. Both two-terminal and four-terminal structures (see Fig.1.) were fabricated in this experiment. For two-terminal structures, carrier density was controlled by a $10\mu\text{m}$ -long Schottky gate placed upon the implanted pattern. For four-terminal structures, carrier density was controlled by illumination followed by a heat cycle. All measurements were carried out by applying a small dc voltage or dc current to the sample.

3.Transport characteristics without magnetic field.

Two-terminal transport characteristics of 100 parallel BPCs placed at intervals of 500nm

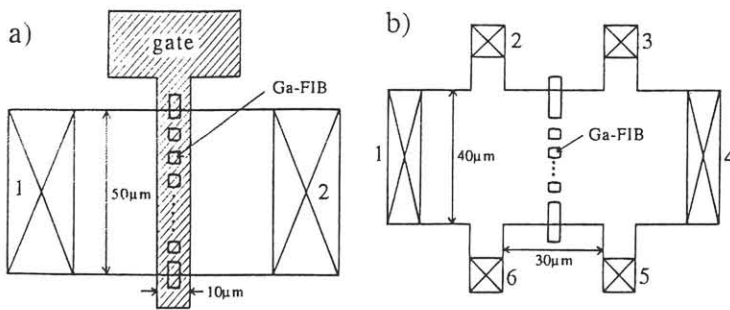


Fig.1 Schematic diagrams showing top view of multiple parallel ballistic point contacts fabricated by Ga-FIB scanning. a) two-terminal structure and b) four-terminal structure. Numbered cross-hatched area represent ohmic contacts.

were measured at 4.2K as a function of gate voltage. Results are shown in Fig.2. Faint step structures were observed in the $I_{ds}-V_g$ characteristics at $B=0T$, and the derivatives, $g_m=dI_{ds}/dV_g$, revealed clear peak structures. In contrast, a single broad peak was observed in g_m for the reference 2-DEG sample. The gate voltage interval of the g_m peaks was about 0.12V. This value corresponds to a Fermi energy variation of about 3meV, which agrees reasonably with subband energy separation in each point contact. Furthermore, measured step structures and g_m characteristics can be calculated by assuming that total conductance of multiple parallel BPCs becomes the sum of the conductances of each of the contacts. Other experiments carried out for 5-100 parallel BPCs at $B=0T$ also support this simple additive rule of conductance in parallel structures.

It is noteworthy that the g_m value in Fig.2a was only slightly degraded by the insertion of parallel BPCs¹⁰. Taking into account a small effective contact width ($W_{eff} \sim 150nm$ per contact interval of 500nm) of the fabricated structure, the g_m value per conductive channel width of multiple parallel BPCs was larger than that of the reference wide 2-DEG sample.

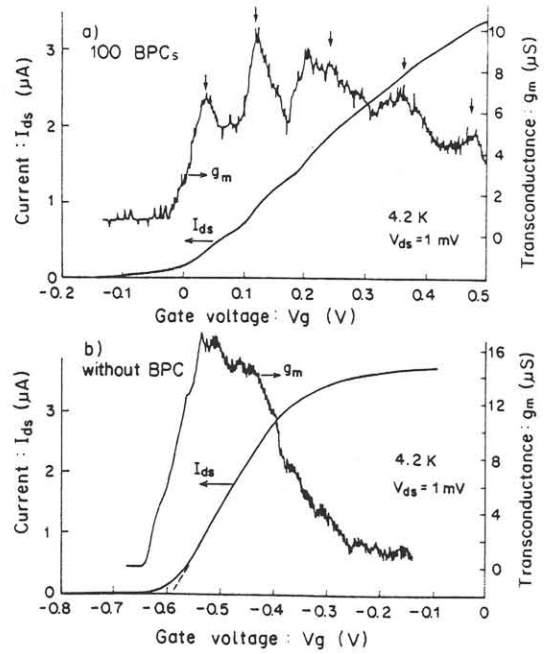


Fig.2 Drain current (I_{ds}) and $g_m=dI_{ds}/dV_g$ as a function of V_g a) for 100 parallel BPCs and b) for the reference sample without implantation. Measurements were carried out at 4.2K under dc drain-to-source bias of 1mV in zero magnetic field.

4. Transport characteristics in magnetic field.

The simple additive rule of conductance in multiple parallel BPCs does not apply in a magnetic field, for multiple parallel BPCs with sufficiently small contact separation. This is due to the novel type of magnetodepopulation made possible by the availability of circulating channels. When several contacts are placed within l_e , the electron motion in a low magnetic field can complete ballistic circulating channels through pairs of contacts. Circulating channels do not contribute to the total current, and therefore result in a decrease in conductance.

Normalized two-terminal conductance was measured as a function of magnetic field and results are shown in Figs. 3 and 4. The number of contacts (N_c) was varied from 1 to 10 and contact separation (L_s) was fixed at 500nm. The Fermi energy (E_f) and number of subbands (i) in each contact were estimated from carrier density and from conductance at

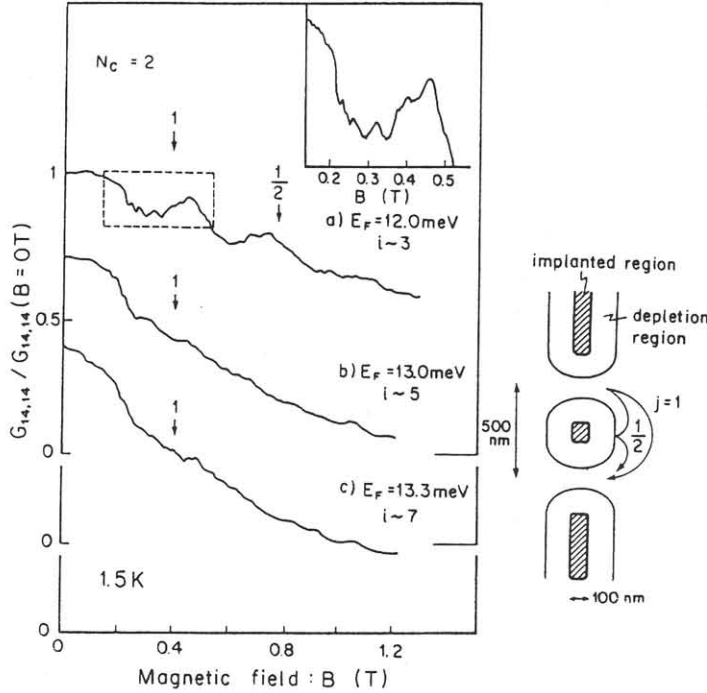


Fig.3 Normalized two-terminal conductance of double parallel BPCs measured as a function of magnetic field. Carrier density (i.e. E_F) and number of subband, i , in each contact were controlled by a combination of illumination and heat cycle. Solid arrows indicate magnetic field where $2l_{cyc}=jL_s$ ($j=1$ and $1/2$). These trajectories are shown in the right hand figure. Inset is the magnification of fine structure in $j=1$ conductance dip in a).

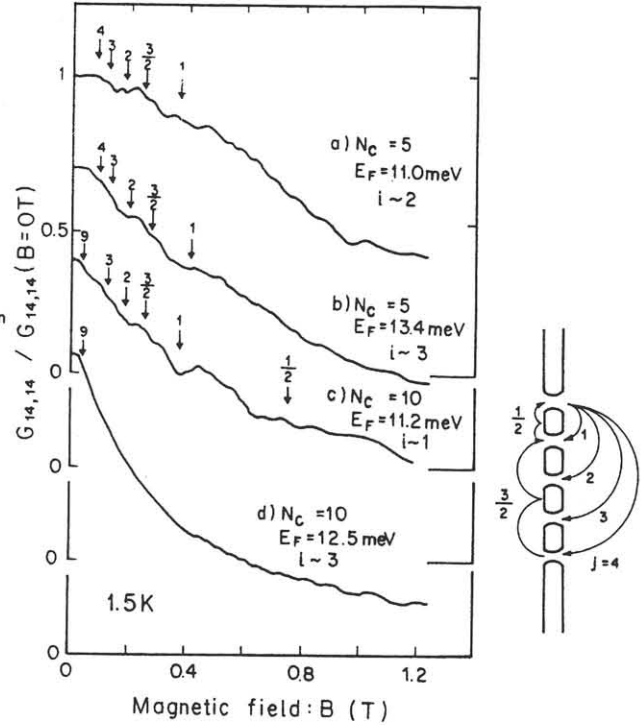


Fig.4 Normalized two-terminal conductance of multiple parallel BPCs measured as a function of magnetic field. N_C is the number of contacts. Solid arrows indicate magnetic field where $2l_{cyc}=jL_s$ ($j=1-4, 9, 1/2, 3/2$). Corresponding trajectories are shown in the right hand figure.

$B=0T$, respectively. Experimental results clearly indicate the following points: 1) A conductance decrease was observed in low magnetic fields where no-depopulation occurs for a single contact. 2) Conductance dips were observed with changing the magnetic field where the electron focusing condition $2l_{cyc}=jL_s$ is satisfied, where l_{cyc} is the cyclotron radius ($l_{cyc}=\sqrt{2m^*E_F/eB}$)^{11,12}. Many kinds of dips, $j=1/2, 1, 3/2, 2, 3$ and 4 , were observed in these experiments (see Fig.4). A fractional j corresponds to trajectories reflected by the depletion region edge. 3) The conductance decrease starts where the magnetic field approximately corresponds to the maximum diameter allowed by the system, $2l_{cyc}=(N_C-1)L_s$. 4) The large contact width (in other words large i) and large number of

contacts enhance the conductance decrease. These observed characteristics demonstrate existence of the novel type of magneto-depopulation accompanying circulating channels in multiple parallel BPCs¹³).

In addition, fine structures were observed in the $j=1$ conductance dip as shown in the inset of Fig.3. These conductance oscillations are explained by an electron wave interference effect in the circulating channel. Unlike the AB-type oscillation reported for high magnetic fields⁹), the trajectory length of the $j=1$ circulating channel is much affected by magnetic field. Therefore, the valley position interval ΔB is not constant but increases with magnetic field.

Finally, four-terminal resistance characteristics of ten parallel BPCs are shown in Fig.5. The two-terminal characteristics of

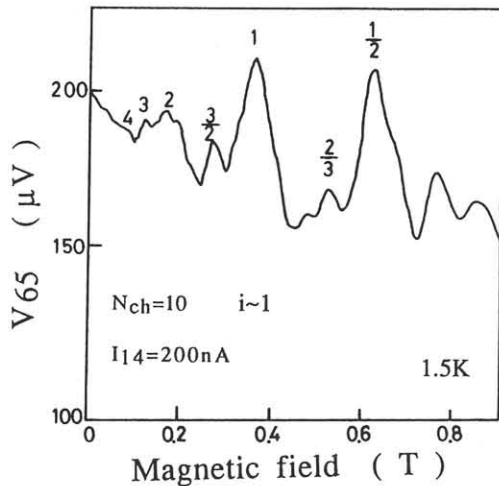


Fig.5 Four-terminal voltage output vs. magnetic field for ten parallel BPCs. Though peak positions of $j=1/2, 2/3$ and 1 are slightly shifted from the calculation using $2l_{\text{cyc}}=jL_s$, resistance peaks corresponding $j=1/2, 2/3, 1, 3/2, 2, 3$ and 4 are clearly observed in this figure.

the same structure were shown in Fig.4c. The depopulation effects discussed above are cancelled by the resistance decrease peculiar to four-terminal measurements¹⁴). Therefore, structures corresponding to different kinds of circulating channels ($j=1/2, 2/3, 1, 3/2, 2, 3$ and 4) are clearly observed in this figure. The same peak height for the $j=1$ and $j=1/2$ peaks, and clear observation of the $j=3/2$ and $2/3$ peaks indicate good specularity of the depletion edge defined by the Ga-FIB scanning and annealing¹⁵).

5. Conclusions

Without magnetic field, total conductance of multiple parallel BPCs is the sum of the conductance of each contact. With magnetic field, the electron motion can complete ballistic circulating channels through pairs of contacts. Activation of these channels depopulate the number of current carrying channels, thus decreasing the total conductance. Furthermore, conductance oscillations corresponding to interference in circulating channels were observed in the double parallel BPCs.

Acknowledgement

I would like to thank T.Saku for preparing high mobility wafers, Dr.Y.Horikoshi and Dr.S.Tarucha for valuable discussions, and Dr.J.R.Phillips for critical reading of this manuscript. I am also indebted to Dr.T.Kimura for his encouragement throughout this work.

References

- 1) B.J.van Wees, H.van Houten, C.W.Beenakker, J.G.Williamson, L.P.Kouwenhoven, D.van der Marel, and C.T.Foxon, Phys. Rev. Lett. **60**. (1988) 848 .
- 2) D.A.Wharam, T.J.Thornton, R.Newbury, M.Pepper, H.Ahmed, J.E.F.Frost,D.G.Hasko, D.C.Peacock, D.A.Ritchie, and G.A.C.Jones, J.Phys.**C21**. (1988) L209 .
- 3) R.E.Behringer, P.M.Mankiewich, G.Timp, R.E.Howard, H.U.Baranger, J.Cunningham, and S.Sampere, J.Vac. Sci. Technol. **B7**. (1989) 2039.
- 4) Y.Hirayama, T.Saku, and Y.Horikoshi, Jpn. J. Appl. Phys. **28**. (1989) L701.
- 5) Y.Hirayama and T.Saku, Appl. Phys. Lett. **54**. (1989) 2556.
- 6) D.A.Wharam, M.Pepper, H.Ahmed, J.E.F.Frost, D.G.Hasko, D.C.Peacock, D.A.Ritchie, and G.A.C.Jones, J.Phys. **C21**. (1988) L887.
- 7) L.P.Kouwenhoven, B.J.van Wees, W.Kool, C.J.P.M.Harmans, A.A.M.Staring, and C.T.Foxon Phys. Rev. **B40**.(1989) 8083 .
- 8) Y.Hirayama and T.Saku, Phys. Rev. **B41**. (1990) 2927 : Y.Hirayama and T.Saku, Solid State Communications, **73** (1990) 113.
- 9) C.G.Smith, M.Pepper, R.Newbury, H.Ahmed, D.G.Hasko, D.C.Peacock, J.E.F.Frost,D.A.Ritchie,G.A.C.Jones and G.Hill, J.Phys.: Condens. Matter **1**. (1989) 6763.
- 10) Y.Hirayama and T.Saku, Jpn. J. Appl. Phys. **29**. (1990) L368.
- 11) H.van Houten, C.W.J.Beenakker, J.G.Williamson, M.E.I.Brockaart, P.H.M.van Loosdrecht, B.J.van Wees, J.E.Mooij, C.T.Foxon and J.J.Harris, Phys. Rev. **B38**. (1989) 8556.
- 12) K.Nakamura, D.C.Tsui, F.Nihey, H.Toyoshima and T.Itoh, Appl. Phys. Lett., **56**. (1990) 385.
- 13) Y.Hirayama and T.Saku, to be published.
- 14) H.van Houten, C.W.J.Beenakker, P.H.M. van Loosdrecht, T.J.Thornton, H.Ahmed, M.Pepper, C.T.Foxon and J.J.Harris, Phys. Rev. **B37**. (1988) 8534.
- 15) S.Nakada, Y.Hirayama, T.Saku, S.Tarucha and T.Horikoshi, to be published.